ACS APPLIED MATERIALS & INTERFACES

Research Article

www.acsami.org

Ultrafiltration of Uranyl Peroxide Nanoclusters for the Separation of Uranium from Aqueous Solution

Ernest M. Wylie,[†] Kathryn M. Peruski,[†] Jacob L. Weidman,[‡] William A. Phillip,[‡] and Peter C. Burns*[,†,§]

[†]Department of Civil and Environmental Engineering and Earth Sciences, University of Notre Dame, Notre Dame, Indiana 46556, United States

[‡]Department of Chemical and Biomolecular Engineering, University of Notre Dame, Notre Dame, Indiana 46556, United States

[§]Department of Chemistry and Biochemistry, University of Notre Dame, Notre Dame, Indiana 46556, United States

Supporting Information

ABSTRACT: Uranyl peroxide cluster species were produced in aqueous solution by the treatment of uranyl nitrate with hydrogen peroxide, lithium hydroxide, and potassium chloride. Ultrafiltration of these cluster species using commercial sheet membranes with molecular mass cutoffs of 3, 8, and 20 kDa (based on polyethylene glycol) resulted in U rejection values of 95, 85, and 67% by mass, respectively. Ultrafiltration of untreated uranyl nitrate solutions using these membranes resulted in virtually no rejection of U. These results demonstrate the ability to use the filtration of cluster species as a means for separating U from solutions on the basis of size. Small-angle X-ray scattering, Raman spectroscopy, and electrospray ionization mass spectrometry confirmed the presence of uranyl peroxide cluster species in solution and were used to characterize their size, shape, and dispersity.

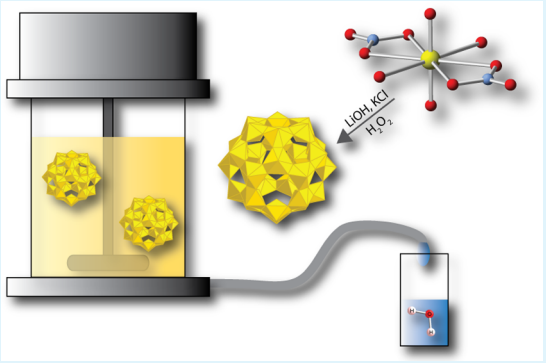

KEYWORDS: *ultrafiltration, uranyl peroxide nanocluster, nuclear technology, membranes, nanoscale control*

1. INTRODUCTION

Uranyl peroxide nanocluster species have been the focus of recent attention because of their rapid self-assembly and persistence in aqueous solution under ambient conditions.[1−5] First discovered in 2005, this class of nanoparticles has grown in size and diversity to ∼40 members that assemble in solution over a wide range of chemical and physical conditions.[6] Most of what is known about these species is gathered from single-crystal X-ray diffraction data. However, electrochemical, thermodynamic, and kinetic studies are currently underway to characterize their properties in solution.[7−11] Their solution properties are of particular interest from both an environmental perspective and an engineering perspective, especially with respect to their assembly and persistence. For example, hydrogen peroxide is a product of the radiation-driven radiolysis of water, and as such, its formation and the subsequent formation of uranyl peroxide species in nuclear waste or during nuclear accidents may be significant.[12,13] Additionally, a uranium waste stream may be treated with hydrogen peroxide to promote the formation of cluster species, which can be removed from solutions using a variety of separation processes.[14,15]

A defining property of the uranyl peroxide nanocluster family is their large size relative to the size of simple aqueous species. Most of the known clusters are composed of more than 18 uranium atoms, resulting in >1 nm species.[5] The cage clusters are typically composed of collections of four-, five-, or six-membered rings of uranium polyhedra (Figure 1). These properties suggest the possibility that persistent aqueous species of uranyl peroxide clusters can be separated from solutions using size-selective ultrafiltration rather than using a process that focuses on extraction of the free molecular uranyl ion.[16] Ultrafiltration processing could be used both to remove the uranium species from a waste stream for purification and to concentrate and collect the purified uranium product for further processing.

Here, we demonstrate that uranyl peroxide species can be separated from aqueous solutions using ultrafiltration. We utilize three commercial ultrafiltration membranes to separate uranyl peroxide nanocluster species, formed by the treatment of aqueous uranyl nitrate with hydrogen peroxide under basic conditions, while monitoring the rate of mass transfer. Chemical and spectroscopic analyses confirm the separation and quantify the efficiency of ultrafiltration.

2. EXPERIMENTAL SECTION

Caution! *While isotopically depleted U was used in these experiments, precautions for handling radioactive materials should be followed.*

2.1. Preparation of Solutions. A 0.5 M stock solution of uranyl nitrate hexahydrate (UN) was prepared by dissolving solid material into ultrapure water with a resistance of 18.2 MΩ cm. The pH of this

Received: October 14, 2013
Accepted: December 6, 2013
Published: December 6, 2013

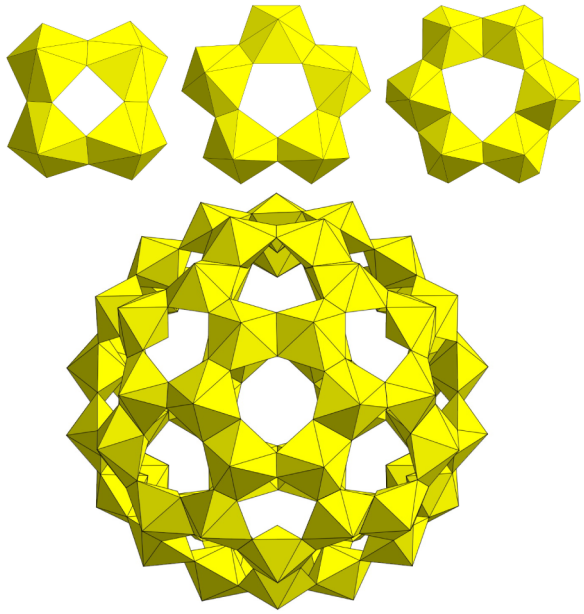

Figure 1. Four-, five-, and six-membered uranyl peroxide and hydroxide bridged rings (top) that are the constituents of many of the uranyl peroxide cage cluster species, such as U60 (bottom).

solution was measured to be 2.68. Aliquots (1 mL) of the UN stock solution were removed and combined with 0.25 mL of 0.4 M KCl, 1 mL of 30% hydrogen peroxide, and 0.7 mL of 2.4 M $LiOH{\cdot}H_2O$, which resulted in a stock solution of uranyl peroxide clusters (UPC) with a pH of 10.18. Because of the high concentrations of the stock solutions, all aliquots taken for each analysis and ultrafiltration experiment were diluted 1:9 in ultrapure water. This dilution results in a slight increase in the pH to 3.48 for the uranyl nitrate solutions and to 10.49 for the uranyl peroxide cluster solutions.

2.2. Ultrafiltration. Three different membranes, purchased from Sterlitech Corp. and Sepro Membranes, were used as received. The membranes manufactured by GE Corp. are members of the GK and GM model lines, and the Sepro membrane is a member of the PS30 model line (Table 1). The membranes were cut using a 1 in. metal hole punch and soaked in refrigerated ultrapure water prior to being used.

Table 1. Characteristics of the Commercial Membranes Used in This Study

manufacturer	GE Water	GE Water	Sepro Inc.
model	GK	GM	PS30
molecular mass cutoff[a]	3K-PEG	8K-PEG	20K-PEG
typical flux (lmh/bar)	418	492	1175
P applied (psi)	35	25	5
stir speed (rpm)	200	200	300

[a]Molecular mass cutoff based on polyethylene glycol (PEG).

Ultrafiltration (UF) experiments were conducted using a Millipore Amicon 8010 10 mL stirred cell. In a standard UF experiment, the stirred cell was filled with 10 mL of a solution at the beginning of the experiment. Then an applied pressure, generated using pressurized nitrogen gas, was used to drive the flow of the solution through the flat sheet membranes. The mass of the solution permeating the membrane was monitored over time and recorded using a Sartorius balance linked directly to a computer. A typical experiment proceeded until 3 mL of the permeate solution had been collected in a scintillation vial for further analysis. Starting and final masses of the liquid-filled stirred cell were recorded to provide mass balance. The observed sieving coefficient, S_O, was used to quantify the ability of the membranes to separate an element from solutions

$$S_O = \frac{c_P}{c_F} \tag{1}$$

where c_P is the solute concentration in the permeate and c_F is the solute concentration in the feed solution.

To minimize the influence of concentration polarization, the stir speeds (ω) used during the ultrafiltration experiments were determined using the relationship developed by Zeman and Zydney for this particular stirred-cell design

$$(kb)/D_i = 0.23(\omega b^2/\nu)^{0.567}(\nu/D_i)^{0.333} \tag{2}$$

where b is the radius of the stirred cell, ω is the angular velocity of the stir bar, ν is the kinematic viscosity of the feed solution, k is the mass transfer coefficient, and D_i is the diffusion coefficient of species i.[17] The dilute solution is assumed to have the same kinematic viscosity as pure water. Values for the diffusion coefficients, D_i, are calculated from the hydrodynamic radii, R_H, of the UPC using

$$D = (k_B T)/(6\pi\mu R_H) \tag{3}$$

where k_B is Boltzmann's constant, T is the temperature, and μ is the viscosity of the solvent (water). Hydrodynamic radii have been previously determined experimentally from dynamic light scattering (DLS) measurements and represent an average particle size in solution.[18] Typical UPC hydrodynamic radii from DLS range from 2 to 5 nm, which leads to diffusion coefficients on the order of 10^{-6} to 10^{-7} cm^2/s for use in the Zeman–Zydney correlation.[17] The stir speed was adjusted to maintain a ratio of the water flux to the mass transfer coefficient of ≤ 1 because this helps to reduce the deleterious effects of concentration polarization. Typical operating conditions are summarized in Table 1.

2.3. Analytical. *2.3.1. Inductively Coupled Plasma Optical Emission Spectroscopy (ICP-OES).* ICP-OES elemental analysis was employed to quantify the concentration of each element in the solutions produced by the filtration process. These concentrations were then used to calculate the sieving coefficient. Elemental concentrations were evaluated using a PerkinElmer Optima 8000 DV ICP-OES instrument with 165–800 nm coverage and a resolution of approximately 0.01 nm for multielemental analysis. Samples were prepared by dilution into 5% nitric solutions. Five standards ranging from 0.5 to 40 ppm were prepared to provide external calibration curves for evaluation of the unknown concentrations. Each standard, blank, and sample was spiked with a 1.0 ppm Y internal standard to monitor matrix effects.

2.3.2. Raman Spectroscopy. Raman spectroscopy was used to determine the presence of a particular species by evaluating the vibrational frequencies of the associated bonds. Spectra were collected from 3 mL aliquots using a Bruker Sentinel system linked via fiber optics to a video-assisted Raman probe equipped with a 785 nm, 400 mW light source and a high-sensitivity, TE-cooled, 1024 × 255 CCD array. The spectra were typically collected at 400 mW for 300 s with a 300 s background over a range from 80 to 3200 cm^{-1}.

2.3.3. Small-Angle X-ray Scattering (SAXS). To determine the size and shape of the uranyl peroxide clusters in solution, their scatter pattern was evaluated using small-angle X-ray scattering. The solutions were introduced into a Bruker Nanostar equipped with a Cu microfocus source, Montel multilayer optics, and a HI-STAR multiwire detector using a continuous flow cell. Background measurements were collected using ultrapure water. The sample data were collected for 3600 s and corrected using background subtraction and integrated over the 2θ range of 0.5–11.5°. DiffracPlus Nanofit was used for modeling.

2.3.4. Electrospray Ionization Mass Spectroscopy (ESI-MS). ESI-MS was utilized to identify and determine the purity of the nanocluster species in solution. Solutions were prepared by centrifugation through 3 kDa molecular mass cutoff Amicon microcentrifugal filters. The retentates were washed with ultrapure water and centrifuged again. The resulting desalted retentates were diluted 1:1000 in ultrapure

water for analyses. Spectra were collected in negative-ion mode using a Bruker micrOTOF-Q II high-resolution quadrapole time-of-flight (Q-TOF) spectrometer (3600 V capillary voltage, 0.8 bar nebulizer gas, 4 L/min dry gas, and 180 °C dry gas temperature). The samples were introduced by direct infusion at a rate of 2.4 μL/min and scanned over the range of m/z 1000−5000 with data averaged over 180 s. MaxEnt was used for the deconvolution of data.[19]

2.3.5. Scanning Electron Microscopy with Energy Dispersive Spectroscopy (SEM/EDS). Following filtration of the UPC solutions, each membrane was gently washed with ultrapure water to remove any residual fluid. The filtered set and a set of unfiltered membrane surfaces were imaged with a Magellan 400 (FEI) field emission scanning electron microscope equipped with a Bruker 123 eV energy dispersive X-ray spectrometer. Prior to being imaged, each membrane was coated with 1.5 nm of iridium. SEM micrographs were collected at 10 kV and 25 pA, and EDS analyses were conducted at 10 kV and 0.4 nA over a 120 μm^2 area for 180−300 s.

3. RESULTS

3.1. Water Flux during Filtration. The linear increase in permeate mass with time indicates that membrane fouling did not occur under the experimental conditions used for any of the ultrafiltration experiments. For the UN solutions, permeate fluxes were measured at $2.37 \times 10^{-4} \pm 9.0 \times 10^{-6}$, $4.34 \times 10^{-4} \pm 1.7 \times 10^{-5}$, and $1.22 \times 10^{-3} \pm 4.82 \times 10^{-4}$ g s^{-1} cm^{-2} for GEGK, GEGM, and PS30, respectively. These flux values are similar to the values measured for pure water of $2.96 \times 10^{-4} \pm 9.0 \times 10^{-6}$, $3.36 \times 10^{-4} \pm 1.7 \times 10^{-5}$, and $1.20 \times 10^{-3} \pm 4.82 \times 10^{-4}$ g s^{-1} cm^{-2}, respectively, at the same applied pressures with errors based on 1.0 psi pressure variations for GEGK and GEGM and 2.0 psi pressure variations for PS30. In contrast, the flux values measured for the UPC solutions are lower than the UN flux values for each membrane ($1.78 \times 10^{-4} \pm 9.0 \times 10^{-6}$, $2.76 \times 10^{-4} \pm 1.7 \times 10^{-5}$, and $(6.0 \pm 4.82) \times 10^{-4}$ g s^{-1} cm^{-2} for GEGK, GEGM, and PS30, respectively). The lower fluxes observed during the filtration of the UPC solutions are likely due to the osmotic pressure that develops due to the retained clusters.[20] The osmotic pressure of these solutions was estimated by assuming that all of the U is in the form of uranyl nanoclusters. On the basis of the measured concentrations reported here, the c_F of the original UPC solution is 0.0165 M. At this concentration, the osmotic pressure can be estimated using the van't Hoff equation

$$\Pi = iRTc_F \quad (4)$$

where i is the van't Hoff factor, R is the gas constant of 0.0821 L atm K^{-1} mol^{-1}, and T is the temperature in kelvin. Assuming the nanoclusters do not dissociate in solution, the van't Hoff factor is equal to 1 and the resulting osmotic pressure, across a membrane with 100% rejection, is equal to 6 psi. This osmotic pressure would reduce the water flux by $1.0-3.0 \times 10^{-4}$ g s^{-1} cm^{-2}, which is comparable to the reductions that were observed in experiments.

3.2. Inductively Coupled Plasma Optical Emission Spectroscopy. Visual inspection of the results of the ultrafiltration experiments gives the first indication that the membranes separate U from solution when the UPC solutions are filtered, but not when the UN solutions are filtered (Figure 2). ICP-OES data indicate that the uranium present in the UN stock solutions passes each membrane virtually unimpeded (Table 2). Sieving coefficients of 0.97, 1.0, and 1.0 for GEGK, GEGM, and PS30, respectively, were calculated for the permeate versus the original concentrations and represent minimal rejection by the membrane. Uranium recovery values

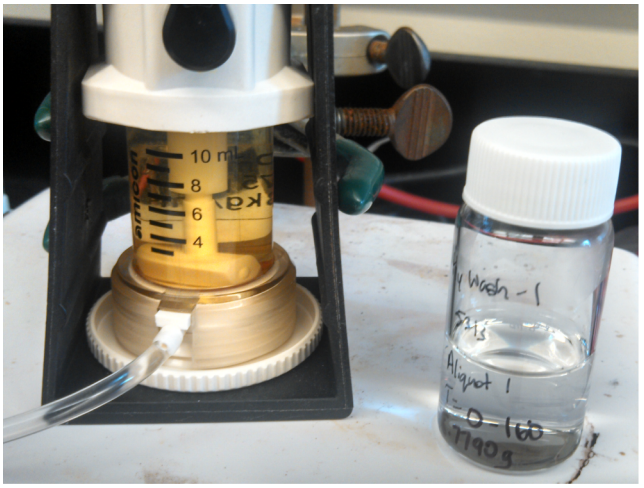

Figure 2. Visual inspection of the retentate and permeate solutions produced during an ultrafiltration experiment suggests that solutions with differing uranium concentrations are produced when the UPC solutions are filtered. The colorless permeate compared to the yellow retentate indicates a significant decrease in the UO_2^{2+} concentration.

of 2.9, 0.5, and 0.3% by mass for GEGK, GEGM, and PS30, respectively, are within the margin of error for the method.

The general trends in the measured uranium concentrations from the UPC experiments contrast sharply with the UN data (Table 2) and are indicative of a large percentage of uranium rejection. This is evident upon examination of the concentration of U in the permeate solutions compared to the concentration of U in the original UPC solution. These values yield sieving coefficients of 0.05, 0.15, and 0.37 and U recovery values of 98.1, 93.7, and 87.4% for GEGK, GEGM, and PS30, respectively, at a 30% stage cut.

The chemical analyses of the UPC solutions also included Li and K concentrations for the original, retentate, and permeate solutions for each ultrafiltration experiment. The Li and K values provide insight about speciation (i.e., which of these elements is likely closely associated with U). The K concentrations suggest that this element is rejected nearly as efficiently as U with sieving coefficients of 0.10, 0.18, and 0.36 for GEGK, GEGM, and PS30, respectively. In contrast, the Li concentrations indicate that a large percentage is not rejected with sieving coefficients of 0.71, 0.80, and 0.84 for GEGK, GEGM, and PS30, respectively. These data indicate that the K^+ is more closely associated with U than Li^+ in the UPC solutions.

3.3. Raman Spectroscopy. Raman spectra are consistent with the chemical analyses, indicating that the separation of U from solution is evident in the UPC solutions while it is absent in the UN control solutions. Figure 3A depicts the Raman shifts for the UN original, retentate, and permeate solutions. The peaks at 870 and 1047 cm^{-1} are assigned to the U−O uranyl and N−O free nitrate stretches, respectively. These shifts remain unaltered in each of the processed solutions, suggesting that uranyl is present at similar concentrations in all of the solutions. Figure 3B depicts the Raman shifts for the UPC original, retentate, and permeate solutions. The peaks at 808, 836, and 1048 cm^{-1} are assigned to the uranyl U−O, uranyl peroxide U−O, and N−O free nitrate stretches, respectively.[21] While the free nitrate stretches are evident in all of the spectra, the uranyl and uranyl peroxide stretches are absent in those of the permeate solutions, indicating their concentrations have

Table 2. ICP-OES Elemental Analyses[a]

GEGK	UN−U	±	UPC−U	±	UPC−Li	±	UPC−K	±
S_O	0.97		0.05		0.71		0.10	
c_R	10844	434	5661	226	439	18	184	7
c_P	10019	401	177	7	280	11	13	0.5
GEGM	UN−U	±	UPC−U	±	UPC−Li	±	UPC−K	±
S_O	1.00		0.15		0.80		0.18	
c_R	10485	419	5420	217	422	17	172	7
c_P	10319	413	603	24	315	13	23	0.9
PS30	UN−U	±	UPC−U	±	UPC−Li	±	UPC−K	±
S_O	1.00		0.37		0.84		0.36	0.10
c_R	10866	435	5424	217	410	16	154	184
c_P	10317	413	1475	59	331	13	47	13
c_F	10348	414	3935	157	396	16	130	5

[a]The sieving coefficient (S_O) is defined as the downstream concentration as a function of the original concentration. Retentate (c_R) and permeate (c_P) concentrations in parts per million are provided for each ultrafiltration experiment for comparison with the original concentrations (c_F).

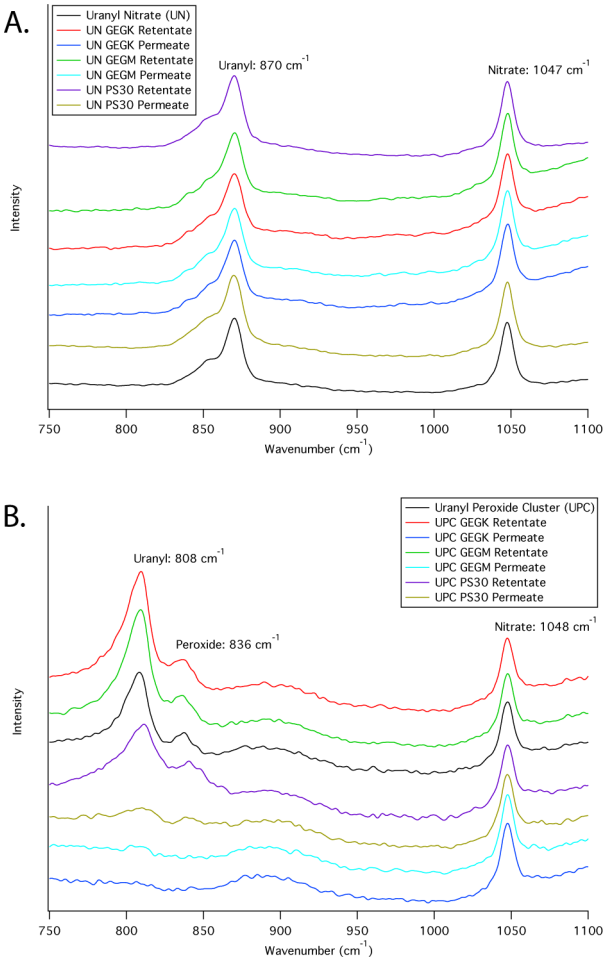

Figure 3. Raman shifts for the UN stock, permeate, and retentate solutions (A) and UPC stock, permeate, and retentate solutions (B).

dropped below the limit of detection for the instrument, presumably as a result of ultrafiltration.

3.4. Small-Angle X-ray Scattering. SAXS data provide important information about the size and shape of the particles in the UN and UPC solutions and provide insight about the concentration distributions observed in the chemical analyses. Figure 4A contains the raw scattering data from the UPC original solution with the calculated curve for a spherical shell model. The agreement between model and experiment suggests that spherically shaped particles with an average outer radius of 9.7 ± 0.2 Å and an average inner radius of 4.5 ± 0.2 Å are present in the UPC original solution. Particles of this size are consistent with the size of uranyl peroxide nanospheres that was previously reported.[5,6,22] In particular, these values correspond well to single-crystal data for clusters with diameters on the order of 2 nm, which is expected because the synthesis method for the UPC solution is similar to the synthesis methods reported for the formation of crystalline products.[22] These data also agree well with the solute size inferred from the ultrafiltration experiments that range from 2.3 to 4.2 nm in diameter (calculations provided in the Supporting Information). Figure 4B shows the raw scattering data for the retentate solution from the UPC GEGK experiment. Similarly, these data suggest spherically shaped particles with an average outer radius of 9.4 ± 0.2 Å and an average inner radius of 4.7 ± 0.2 Å are present in the retentate. These particles are also present in the GEGM and PS30 retentate. Nanosized particles are not indicated in the scattering patterns for the UN solutions, the UPC GEGK, and the UPC GEGM permeates (Figure 4C). However, they are present in the PS30 permeate as revealed by Figure 4D.

3.5. Electrospray Ionization Mass Spectroscopy. The mass spectrum for the UN original solution indicates that particles with large m/z values are absent from solution, as expected (Figure 5). However, particles with high m/z values are present in the UPC original and retentate solutions, while they are absent from the permeate solutions. Several broad peaks between m/z 1200 and 2000 demonstrate that the UPC original and retentate solutions are likely polydisperse with at least two large species in solution assuming no fragmentation in the spectrometer. One species, with a molecular mass of ~8 kDa, can be assigned to the broad peaks at m/z 1270, 1520, and 1950 with charge states of −6, −5, and −4, respectively. A larger species, with a molecular mass of ~10 kDa, can be assigned to peaks at m/z 1390 and 1600 with charge states of −7 and −6, respectively. A third species may also be present with a molecular mass of ~11 kDa if peaks at m/z 1490 and 1750 are assigned charge states of −7 and −6, respectively. These spectra are consistent with U-24, U-28, and U-32 nanocages that have molecular masses of 7−11 kDa based on published formulae.[6] This is particularly interesting considering the U-28 nanocage is templated by K^+ while U-24 is templated

dx.doi.org/10.1021/am404520b | ACS Appl. Mater. Interfaces 2014, 6, 473−479

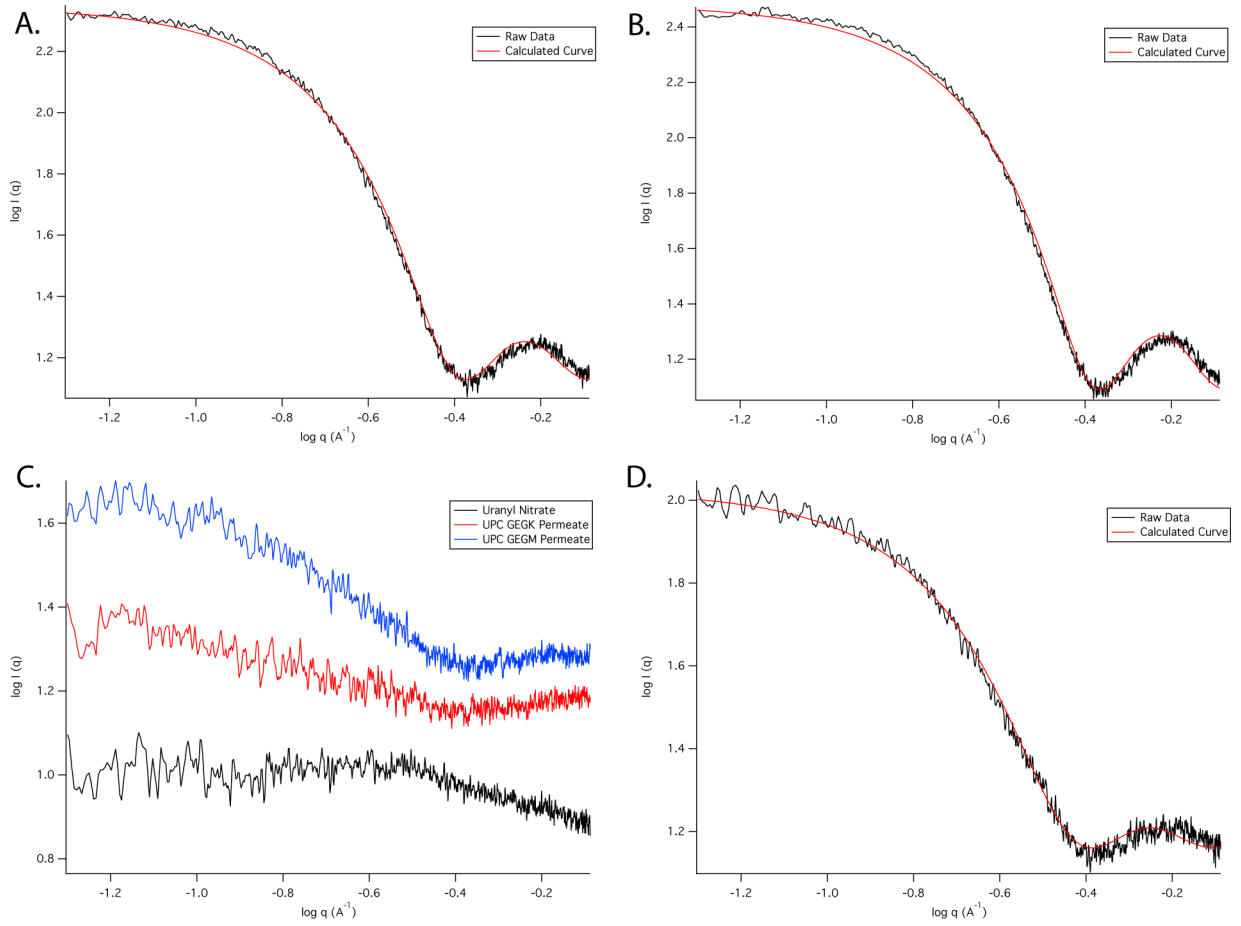

Figure 4. Log/log plot of the SAXS data collected for the UPC stock solution with a calculated fit for a spherical shell model with an outer radius of 9.7 Å and an inner radius of 4.5 Å (A), the UPC GEGK retentate solution with a calculated fit for a spherical shell model with an outer radius of 9.4 Å and an inner radius of 4.7 Å (B), the UN, UPC GEGK permeate, and UPC GEGM permeate solutions (C), and the UPC PS30 permeate solution with a calculated fit for a spherical shell model with an outer radius of 10.1 Å and an inner radius of 4.3 Å (D).

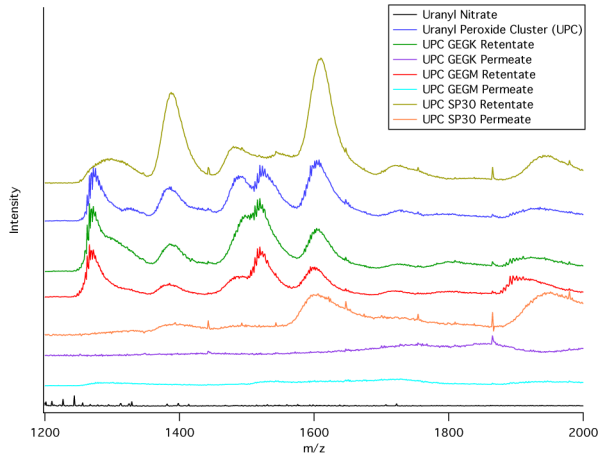

Figure 5. ESI-MS traces for the UN stock, UPC stock, and UPC retentate and permeate solutions.

by Li^+. In the context of the chemical data presented here, it is possible that the U-28 nanocage is a major constituent of the UPC solutions.

4. DISCUSSION

This work demonstrates that treating a pure uranyl nitrate stream with hydrogen peroxide, lithium hydroxide, and potassium chloride results in the formation of discrete, nanoscale, spherical uranyl peroxide particles, which can be filtered from solution using size-selective membranes. The SAXS data for the UPC-containing solutions can be fit to spherical shell models with outer diameters of ∼2 nm, a value that agrees well with both single-crystal data and solute rejection calculations. The deviation between the average cluster sizes determined by the different techniques and imperfections in the fit of the model to data are likely the result of polydispersity. ESI-MS data confirm this polydispersity, with at least two large species assigned to the MS peaks. Regardless, these data indicate that the U-containing species in UPC solutions have a high molecular mass relative to that of the simple aqueous species found in uranyl nitrate solutions.

Under the experimental conditions utilized here, the assembly of uranyl peroxide clusters accounts for nearly all of the uranium in solution. Evidence that supports this idea is provided by the ultrafiltration experiments for pure uranyl nitrate streams, which result in virtually no uranium rejection. One might argue that the increased pH and ionic strength of the UPC solutions compared to those of the pure uranyl nitrate solution result in uranium being adsorbed by the membrane surface. This could also lead to the low U concentrations that were measured for the UPC permeate solutions. However, the water flux data give no evidence of uranium species being adsorbed by the membrane surfaces during the stirred cell

dx.doi.org/10.1021/am404520b | ACS Appl. Mater. Interfaces 2014, 6, 473−479

experiment. Adsorption would likely lead to fouling, and the flux would decrease over time, causing the mass versus time curves to deviate from their observed linear character. This did not occur. Furthermore, mass balances on the uranium in the original solution, the retentate, and the permeate indicate that the majority of the U remains in solution (i.e., it is not adsorbed by the membrane). Finally, EDS analyses and SEM micrographs of the membrane surfaces subsequent to filtration of UPC species indicate the absence of U on the membrane surface and no significant alteration of the surface structures compared to virgin membrane surfaces, respectively.

Increasing the pH of a uranyl nitrate solution to values measured in the UPC stock will result in the precipitation of uranyl hydrolysis products in the absence of a complexing agent.[23] This impairs our ability to test pure uranyl nitrate solutions at the same pH values as the UPC stock. When excess carbonate is present, uranyl carbonate species can persist in solution at high pH. Previous work suggests that uranyl peroxide−carbonate species can be prepared with hydrogen peroxide and excess carbonate at pH values similar to that of the UPC stock for specific separation applications.[14,15,24] However, no evidence of uranyl carbonate or free carbonate is apparent in the UPC Raman spectra, so if they are present, they are minor species attributed to the introduction of atmospheric carbonate.

Indeed, there is also no evidence that the small amount of uranium that passes through the membranes in the treated solutions consists of free uranyl ions. Detection of large, spherically shaped species in the PS30 permeate suggests that the U measured in each permeate may be attributed to membrane rejection inefficiency. The permeate solutions may also contain monomeric or dimeric uranyl peroxide species or nanocluster fragments. At this point, the low U concentrations present in the UPC GEGK and GEGM permeate solutions preclude determination of the speciation.

5. CONCLUSION

This study suggests it may be possible to design an ultrafiltration operation to recover U from solution by exploiting the difference in size between UPC and smaller solutes in solution. Similar to the design of many membrane operations, this will entail balancing throughput and selectivity. The results of this study begin to suggest what some key characteristics of a membrane for the process might be. On the basis of the size of the particles in solution, and the three different membrane pore sizes that were utilized in this study, we suspect that membranes with molecular mass cutoff values lower than 5K-PEG will give ≥90% rejection by mass of the U in UPC. Membranes with pore sizes of up to 20K-PEG molecular mass cutoff may still yield rejection values of >50% with dramatic increases in permeability relative to the smaller pore sizes. These data will aid in the design and synthesis of new membrane materials designed specifically for processing UPC solutions.

■ ASSOCIATED CONTENT

Supporting Information

Transport data, mass balance data, Raman spectra, ESI-MS spectra, solute transport size equations, SEM micrographs and EDS spectra, and ICP-OES standard curves. This material is available free of charge via the Internet at http://pubs.acs.org.

■ AUTHOR INFORMATION

Corresponding Author

*E-mail: pburns@nd.edu.

Author Contributions

All authors contributed equally to this work.

Notes

The authors declare no competing financial interest.

■ ACKNOWLEDGMENTS

This research is funded by the Office of Basic Energy Sciences of the U.S. Department of Energy as part of the Materials Science of Actinides Energy Frontiers Research Center (DE-SC0001089). Chemical analyses were conducted at the Center for Environmental Science and Technology at the University of Notre Dame. Electrospray ionization mass spectra were collected at the Mass Spectrometry and Proteomics Facility at the University of Notre Dame. Raman spectra were collected at the Materials Characterization Facility of the Center for Sustainable Energy at the University of Notre Dame.

■ ABBREVIATIONS

UF, ultrafiltration
UN, uranyl nitrate solution
UPC, uranyl peroxide cluster solution
PEG, polyethylene glycol
SAXS, small-angle X-ray scattering
ICP-OES, inductively coupled plasma optical emission spectrometry
ESI-MS, electrospray ionization mass spectrometry
SEM/EDS, scanning electron microscopy/energy dispersive spectroscopy

■ REFERENCES

(1) Kubatko, K.; Gunderson, K. M.; Antonio, M.; Burns, P. C.; Soderholm, L. *Mater. Res. Soc. Symp. Proc.* **2006**, *893*, 387−392.
(2) Sigmon, G. E.; Ling, J.; Unruh, D. K.; Moore-Shay, L.; Ward, M.; Weaver, B.; Burns, P. C. *J. Am. Chem. Soc.* **2009**, *131*, 16648−16649.
(3) Nyman, M.; Rodriguez, M. A.; Campana, C. F. *Inorg. Chem.* **2010**, *49*, 7748−7755.
(4) Sigmon, G. E.; Burns, P. C. *J. Am. Chem. Soc.* **2011**, *133*, 9137−9139.
(5) Qiu, J.; Burns, P. C. *Chem. Rev.* **2013**, *113*, 1097−1120.
(6) Burns, P.; Kubatko, K.; Sigmon, G.; Fryer, B.; Gagnon, J.; Antonio, M.; Soderholm, L. *Angew. Chem., Int. Ed.* **2005**, *44*, 2135−2139.
(7) Armstrong, C. R.; Nyman, M.; Shvareva, T.; Navrotsky, A. *Abstracts of Papers*; American Chemical Society: Washington, DC, 2011; Abstract 241.
(8) Gil, A.; Karhanek, D.; Miro, P.; Antonio, M. R.; Nyman, M.; Bo, C. *Chem.—Eur. J.* **2012**, *18*, 8340−8346.
(9) Nyman, M.; Alam, T. M. *J. Am. Chem. Soc.* **2012**, *134*, 20131−20138.
(10) Johnson, R. L.; Ohlin, C. A.; Pellegrini, K.; Burns, P. C.; Casey, W. H. *Angew. Chem., Int. Ed.* **2013**, *52*, 7464−7467.
(11) Oliveri, A. F.; Elliott, E. W.; Carnes, M. E.; Hutchison, J. E.; Johnson, D. W. *ChemPhysChem* **2013**, *14*, 2655−2661.
(12) Forbes, T. Z.; Horan, P.; Devine, T.; McInnis, D.; Burns, P. C. *Am. Mineral.* **2011**, *96*, 202−206.
(13) Armstrong, C. R.; Nyman, M.; Shvareva, T.; Sigmon, G. E.; Burns, P. C.; Navrotsky, A. *Proc. Natl. Acad. Sci. U.S.A.* **2012**, *109*, 1874−1877.
(14) Chung, D.; Seo, H.; Lee, J.; Yang, H.; Lee, E.; Kim, K. *J. Radioanal. Nucl. Chem.* **2010**, *284*, 123−129.

(15) Soderquist, C. Z.; Johnsen, A. M.; McNamara, B. K.; Hanson, B. D.; Chenault, J. W.; Carson, K. J.; Peper, S. M. *Ind. Eng. Chem. Res.* **2011**, *50*, 1813−1818.
(16) Bohinc, K.; Reščič, J.; Dfreche, J.; Lue, L. *PhysChemComm* **2013**, *117* (37), 10846−10851.
(17) Zeman, L. J.; Zydney, A. L. In *Microfiltration and ultrafiltration: Principles and applications*; Marcel Dekker: New York, 1996; p 618.
(18) Wallace, C. M. Solution and Aggregation Behavior of the U60 Nanocluster and Post-Detonation Nuclear Forensic Analysis of Trinitite. Ph.D. Dissertation, University of Notre Dame, Notre Dame, IN, 2013.
(19) Ferroge, A. G.; Seddon, M. J.; Skilling, J.; Ordsmith, N. *Rapid Commun. Mass Spectrom.* **1992**, *6*, 765−770.
(20) Kedem, O.; Katchalsky, A. *J. Gen. Physiol.* **1961**, *45*, 143−179.
(21) Qiu, J.; Nguyen, K.; Jouffret, L.; Szymanowski, J. E. S.; Burns, P. C. *Inorg. Chem.* **2013**, *52*, 337−345.
(22) Sigmon, G.; Unruh, D.; Ling, J.; Weaver, B.; Ward, M.; Pressprich, L.; Simonetti, A.; Burns, P. *Angew. Chem., Int. Ed.* **2009**, *48*, 2737−2740.
(23) Clark, D.; Hobart, D.; Neu, M. *Chem. Rev.* **1995**, *95*, 25−48.
(24) Kim, K.; Chung, D.; Yang, H.; Lim, J.; Lee, E.; Song, K.; Song, K. *Nucl. Technol.* **2009**, *166*, 170−179.